Online Transient Stability Assessment Implementing the Weighted Least-square Support Vector Machine with the Consideration of Protection Relays

Amir Hossein Poursaeed and Farhad Namdari

***Abstract*—Weighted least-square support vector machine (WLS-SVM) is proposed in this research as a real-time transient stability evaluation method using the synchrophasor measurement received from phasor measurement units (PMUs). This method considers the directional overcurrent relays (DOCRs) for the transmission system, whereas in previous studies, the effect of protective mechanisms on the transient stability was largely ignored. When protective relays are activated in power system, the configuration of the power system is altered to mitigate the risk of the power system becoming unstable. The present study considers the operation of DOCRs in transmission lines for the transient stability so that the proposed method can respond to changes in the configuration of the case study system. In addition, WLS-SVM is employed for an online assessment of the transient stability. WLS-SVM not only is effective in response due to its faster speed, but also is resistant to noise and has excellent performance against the measurement errors of PMUs. To extract the characteristics of the vectors that are fed into the WLS-SVM algorithm, principal component analysis is used. The findings of the suggested technique reveal that it has higher accuracy and optimum performance, as compared to the extreme learning machine method, the adaptive neuro-fuzzy inference system method, and the back-propagation neural network method. The proposed technique is validated in the New England 39-bus system and the IEEE 118-bus system.**

***Index Terms*—Transient stability assessment, weighted least-square support vector machine, directional overcurrent relay, phasor measurement unit.**

Received: January 30, 2024
Accepted: July 20, 2024
Published Online: January 1, 2025
Amir Hossein Poursaeed is with the Department of Electrical Engineering, Faculty of Engineering, Lorestan University, Khorram Abad 465, Iran (e-mail: poursaeed.ah@fe.lu.ac.ir).
Farhad Namdari (corresponding author) is with the Department of Engineering, Faculty of Environment, Science, and Economy, University of Exeter, Streatham Campus, Exeter, Devon, EX4 4QF, UK (e-mail: f.namdari@exeter.ac.uk).
DOI: 10.23919/PCMP.2023.000032

I. Introduction

A. Aim and Scope

The stability of power systems is regarded as one of the most critical factors for ensuring the networks' secure functioning, since the primary cause of significant power outages is their instability [1]. Historically, transient stability has been an essential component of power systems. Therefore, a significant portion of the electric power industry has focused on power system stability as a primary area of concern [2]. With the continual expansion and improvement of phasor measurement units (PMUs), operators can now use the wide-area measurement system to take quicker preventative steps, thereby increasing stability [3].

B. Related Works

Transient stability, a key aspect of power system stability, has been extensively studied in recent years. With the existing strategies and technological development, the power systems are swiftly evolving, reflecting significant progress in this area. However, this poses new challenges for which innovative solutions are required. Generally, several categories have been proposed for the evaluation of the transient stability of power systems, whereas time-domain, frequency-domain, energy function-based, curve-fitting, and machine-learning methods are among the solutions. While these methods provide a strong basis, their contributions pave the way for new challenges in the transient stability prediction, particularly under the dynamics of modern power grids.

Using time-domain techniques, the transient stability analysis takes into account the system's nonlinear nature, in which the system's differential-algebraic equations can be solved [4]. Despite its unparalleled accuracy and high fidelity in capturing the complex dynamics of power systems, the time-domain-based technique has a large computational cost. Therefore, this necessitates methods that combine the precision of time-domain analysis with the speed required for real-time decision-making [5], such as those that can be applied online. Frequency-domain approaches evaluate

the transient stability by linearizing the nonlinear equations of the system [6]. This approach is more computationally efficient than the time-domain analysis since it is easy to implement. The method's primary drawback is that only one operating point is credible, which prevents it from evaluating with high accuracy when the operational state is changed. Given this limitation, it is necessary for the approaches to maintain their high accuracy across diverse system states without excessive simplification of system dynamics [7]. Therefore, researchers have started using methods based on energy function, known as direct methods, in which a system is only considered stable if its energy is positive and its energy derivative is not positive with regard to time [8]. These approaches determine the system's stability status by comparing the transient energy to the potential energy computed at the unstable operating point [9]. Although these techniques are independent of any modifications to the system's nonlinear equations, thus credible for all operating points, they require more time to establish the stability state than other techniques [10]. Methods that reduce setup time while preserving the strength of direct methods remain a research interest. Therefore, predicting the stability of a power grid via extrapolation, which is the goal of curve-fitting techniques, has become popular recently to overcome the problem of other approaches [11]. In addition, it has a low computing complexity and no need for network reduction, and is less reliant on the topology of the network [12]. However, it lacks the ability to integrate the operational characteristics of specific power system components, such as protection systems, into their stability assessments.

In recent times, the utilization of machine learning has proven to be advantageous in assessing transient stability, outperforming traditional mathematical modeling techniques employed in the power grid analysis [13]. Artificial neural networks (ANN), extreme learning machines (ELM), decision trees (DT), fuzzy logic, adaptive neuro-fuzzy inference systems (ANFIS), and support vector machines (SVM) are employed in conjunction with PMUs to ensure that the rotor angles within a specified network remain within acceptable bounds [14]. The utilization of ANNs can be advantageous in estimating transient stability with speed and accuracy, as they possess a strong capability to identify patterns between input and output data, under both normal and abnormal operating conditions [15]. However, ANNs pose significant challenges due to their time-consuming nature and the need for extensive datasets for effective training. In [16], ELM is used to determine the transient stability state because it requires less time to train. Nevertheless, determining the number of hidden layer neurons, weight matrix, and activation function is one of the challenges of using ELM. DTs can be utilized to address the limitations associated with ELMs [17], though it is necessary to reduce the dimensions of the input vector before training DTs [18]. Due to their susceptibility to overfitting issues and their sensitivity to noise, DTs are commonly ignored, whereas researchers tend to utilize fuzzy logic and its applications to develop controllers that enhance the transient stability [19]. To mitigate the imprecision of fuzzy systems, ANFIS has been employed for online transient stability assessment [20] since ANFIS combines the advantageous characteristics of both ANNs and fuzzy logic. Nevertheless, ANFIS is accompanied by certain challenges related to dimensionality, location, and the type of membership function [21]. SVMs address these challenges in the context of time series prediction and in various status classifications, exhibiting strong performance. Consequently, SVMs are considered as the best choice for accurately forecasting a transient stability evaluation index, and for classifying it as stable or unstable [22]. Nevertheless, SVMs, similar to other machine learning techniques, require a user to perform feature extraction to enhance the system's performance when dealing with high-dimensional data [23]. This process is crucial for selecting relevant features that contribute to more accurate predictions, although deep learning obviates the necessity for feature extraction, as this process is inherently incorporated within the framework [24].

In the above-mentioned studies, the inability to conduct real-time testing of the proposed method has resulted in a lack of viable solutions for its real-time implementation. Nevertheless, these methodologies are susceptible to the influence of noise. To deal with this problem, it is imperative to implement a real-time monitoring system that considers the influence of measurement inaccuracies associated with PMUs on transient stability [25]. Therefore, such machine learning models are in a substantial data-driven manner. So far, no study has sufficiently addressed the incorporation of detailed power system operational mechanisms, including the nuances of protection relay activation. Such gaps, therefore, underline an emerging need for sophisticated machine learning models which are not only data-efficient but also informed by the physical operations of power systems.

C. Contribution

This study presents a novel approach to address the identified gaps and advance the frontier of transient stability assessment. In this work, real-time monitoring and prediction of transient stability of power systems is evaluated by means of weighted least-square support vector machine (WLS-SVM). Moreover, the present study takes into account the effects of directional over current relays (DOCRs) on the transient stability. This paper presents the following key contributions that address the identified gaps in the transient stability prediction and assessment.

1) Attention to system configuration changes emanating from the operation of DOCRs, which had not been previously accounted for.

2) Including the effects of DOCRs on the transient stability in the transmission system, which are critical

factors that influence the response of the system to disturbances.

3) The use of linear programming (LP) for finding the best coordination among DOCRs to avoid wrong setting of relays and the consequent maloperation of DOCRs, which could ultimately lead to the wrong operation of relays, power outages and system collapses.

4) The calculation of the online transient stability by means of WLS-SVM for effective online study with several input characteristics, including high dimensionality and fast prediction, memory saving, improved accuracy, generalizability, and resistance to measurement errors.

5) The use of all available active-reactive power, voltage amplitude, and phase angle data for the training of WLS-SVM after the dimension reduction of the dataset with principal component analysis (PCA) to keep the learning accuracy of the model in harmony with its speed.

6) Comparison between the results obtained from the proposed WLS-SVM method and those obtained from ELM, ANFIS, and back-propagation neural network (BPNN) methods.

7) Validation of the proposed approach over the New England 39-bus and IEEE 118-bus systems to demonstrate the practicability and effectiveness of the proposed approach in practical systems.

D. Organization

The remainder of the paper is structured as follows. Section II describes the transient stability assessment index and optimal coordination among DOCRs. Section III focuses on the structure of WLS-SVM, while Section IV presents the proposed method. Section V deals with simulation results and discussions about the comparison of the proposed method with ELM, ANFIS, and BPNN approaches. Finally, Section VI presents the conclusion.

II. Problem Formulation

This section describes the mathematical modeling and problem expression. First, the concept of transient stability and the corresponding online evaluation index are presented. Then, the overcurrent protection problem and DOCRs optimum coordination problem are represented via LP.

A. Transient Stability Index

A power system is said to be stable in terms of transient stability if it can maintain its synchronism when it is disrupted by a significant disturbance, e.g., a fault, and then recover from it. Rotor angles and generator speeds are directly affected by external disturbances as a result of power imbalances. Therefore, the transient stability of the power systems can be determined by monitoring the generator rotor angles.

Since this paper intends to monitor the power system stability in an online manner while examining the overcurrent protection impact on the transient stability, the present study needs to assess the transient stability in real-time. Unlike other aspects of power system stability that have many online assessment indices, few transient stability assessment indices can evaluate the transient stability in real-time. In [26], a fast index with high computational simplicity is proposed for the online assessment of transient stability, expressed as:

$$i_{\mathrm{TSI}} = \frac{360 - \delta_{\max}}{360 + \delta_{\max}} \tag{1}$$

where i_{TSI} refers to the transient stability index; the largest difference in the rotor angles between the two generators, expressed in absolute terms, is represented by $\delta_{\max}$, taking into account in the post-fault period. The system is stable as long as i_{TSI} is positive, while if i_{TSI} has a negative value, the system is considered unstable.

B. Optimal Coordination Between the DOCRs Problem

In power systems, the most prevalent protection strategy is the overcurrent protection. DOCRs are either the primary or backup protections for transmission lines, busbars, generators, motors, and transformers. Coordination between DOCRs is a vital aspect to ensure a protective system's reliability, selectivity, speed, sensitivity, and stability [27].

The optimum coordination between DOCRs is seen as a minimization of the objective function for a basic electric power system depicted in Fig. 1, expressed as:

$$t_{\mathrm{op}} = \sum_{i=1}^{n} t_i = \sum_{i=1}^{n} \left(\frac{0.14 T_i}{\left(\frac{I_{\mathrm{f}_i}}{I_{\mathrm{pu}_i}} \right)^{0.02} - 1} \right) \tag{2}$$

where t_{op} represents the total time of the operation of the main relays; t_i represents the amount of time that the relay i has been operating; n represents the total number of main relays; T_i represents the time multiplier setting of the relay i; while the pickup current of the relays is I_{pu}, which is chosen as the maximum load current multiplied by 1.5 in this study; additionally, I_{f} denotes the fault current which is being delivered by the main relay.

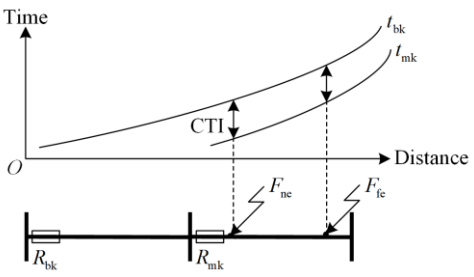

Fig. 1. The structure of primary and backup pairs.

The computation of the global optimum values for T_i is the outcome of the optimization process, as a part of the objective function of optimal coordination. T_i is also constrained in a way that it may serve as one of the optimization problem's constraints:

$$0.1 \leqslant T_i \leqslant 1.1 \tag{3}$$

Furthermore, to avoid the mis-coordination between the main and backup pairs, a time interval has to be taken into account for both far-end and near-end faults, i.e.:

$$t_{bk}(F_{\text{ne}}) - t_{mk}(F_{\text{ne}}) \geqslant t_{\text{CTI}} \tag{4}$$

$$t_{bk}(F_{\text{fe}}) - t_{mk}(F_{\text{fe}}) \geqslant t_{\text{CTI}} \tag{5}$$

where t_{CTI} stands for the coordination time interval, which in this study is taken to be 0.25 s; furthermore, for the relay pairs k, the operation times of the primary and backup relays are t_{mk} and t_{bk}, respectively; additionally, the near-end and far-end fault positions are denoted by F_{ne} and F_{fe}.

III. Weighted Least Squares Support Vector Machine

Due to its speed and accuracy, WLS-SVM can be regarded as one of the best methods for forecasting purposes. The output of WLS-SVM not only results in accurate predictions of any noise for regression, but also obviates the use of all datasets to estimate a particular operating state of the power grids [28]. The target values are predicted by means of the training datasets, specified as $\{(x_1, y_1), \cdots, (x_n, y_n)\}, x_i \in \mathbb{R}^n$, where the number of samples is denoted by n, while x and y are the predictors and target data, respectively.

To predict the transient stability status, different predictors are considered, and they are expressed as x in this paper. To determine the transient stability, the value of i_{TSI} for the sample i is considered to be y. The optimization problem aims to find a solution which minimizes the objective function, shown as:

$$J(\boldsymbol{\omega}, e_i) = \frac{1}{2}\|\boldsymbol{\omega}\|^2 + \frac{1}{2}\gamma\sum_{i=1}^{n} v_i {e_i}^2 \tag{6}$$

where J is the fitness function which takes into account a regularization item as the first term, and the sum squared error for the second term in (6); moreover, $\boldsymbol{\omega}$ represents the weight vector; γ is considered to be a positive penalty factor; e_i stands for the training regression error; and the weighting factor for WLS-SVM is denoted by v_i. The constraint of this optimization problem is represented by:

$$y_i = \boldsymbol{\omega}^{\mathrm{T}}\boldsymbol{\Omega}(x_i) + b + e_i \tag{7}$$

where $\boldsymbol{\Omega}(x_i)$ is considered a transfer function which translates the input space to a space with a larger number of dimensions; while the bias is denoted by b.

The above problem can be solved by forming the Lagrange function, as:

$$L(\boldsymbol{\omega}, b, e_i; \alpha_i) = J(\boldsymbol{\omega}, e_i) + \sum_{i=1}^{n}\alpha_i\left[y_i - \boldsymbol{\omega}^{\mathrm{T}}\boldsymbol{\Omega}(x_i) - b - e_i\right] \tag{8}$$

where α_i is the set of Lagrange multipliers. For the linear equation shown in (8), the Karush-Kuhn-Tucker conditions can be found as:

$$\begin{aligned}
&\frac{\partial L}{\partial \boldsymbol{\omega}} = 0 \rightarrow \boldsymbol{\omega} = \sum_{i=1}^{n}\alpha_i\boldsymbol{\Omega}(x_i)\\
&\frac{\partial L}{\partial \alpha_i} = 0 \rightarrow y_i = \boldsymbol{\omega}^{\mathrm{T}}\boldsymbol{\Omega}(x_i) + b + e_i\\
&\frac{\partial L}{\partial b} = 0 \rightarrow \sum_{i=1}^{n}\alpha_i = 0\\
&\frac{\partial L}{\partial e_i} = 0 \rightarrow \alpha_i = \gamma v_i e_i
\end{aligned} \tag{9}$$

Eliminating $\boldsymbol{\omega}$ and e_i yields:

$$\begin{bmatrix} 0 & (\boldsymbol{I}_n)^{\mathrm{T}} \\ \boldsymbol{I}_n & \boldsymbol{\Phi} + \dfrac{\boldsymbol{I}}{\gamma \boldsymbol{v}} \end{bmatrix}\begin{bmatrix} b \\ \alpha \end{bmatrix} = \begin{bmatrix} 0 \\ y \end{bmatrix} \tag{10}$$

where $\boldsymbol{I}_n = (1,1,\cdots,1)^{\mathrm{T}}$; $\boldsymbol{\alpha} = (\alpha_1, \alpha_2, \cdots, \alpha_n)$; $\boldsymbol{y} = (y_1, y_2, \cdots, y_n)$; $\boldsymbol{\Phi} = \boldsymbol{\Omega}(x_i)^{\mathrm{T}}\boldsymbol{\Omega}(x_j)$; $\boldsymbol{v} = \mathrm{diag}(v_1, v_2, \cdots, v_n)$; and the unit matrix is denoted by $\boldsymbol{I}$. Therefore, the predicted values can be found by solving:

$$y_{\text{P}}(x) = \sum_{i=1}^{n}\alpha_i K(x, x_i) + b \tag{11}$$

where $y_{\text{P}}(x)$ is the predicted values; and the kernel function is represented by $K(x, x_i)$. The present study uses the radial basis function (RBF) kernel function, stated as:

$$K(x, x_i) = \exp\left(\frac{-|x - x_i|^2}{2\sigma^2}\right) \tag{12}$$

where σ represents the kernel function's width. Finally, v_i can be obtained by:

$$v_i = \begin{cases} 1, & \left|\dfrac{e_i}{s}\right| \leqslant c_1 \\ \dfrac{c_2 - \left|\dfrac{e_i}{s}\right|}{c_2 - c_1}, & c_1 \leqslant \left|\dfrac{e_i}{s}\right| \leqslant c_2 \\ 10^{-4}, & \text{otherwise} \end{cases} \tag{13}$$

where s represents the standard deviation, which can be defined as $s = 1.483 e_{\text{MAD}}(e_i)$; it should be noted that the values for the parameters c_1 and c_2 would often be 2.5 and 3; while e_{MAD} is the median absolute deviation, described as:

$$e_{\text{MAD}}(e_i) = \text{median}(|e_i - \text{median}(e_i)|) \tag{14}$$

IV. The Presented Methodology for Online Transient Stability Assessment

The present study assumes that the real-time synchrophasor data of active and reactive powers, voltage amplitudes, and phase angles of the load buses are received from PMUs. These values should be used as the input vectors for the proposed approach to predict i_{TSI} in an online manner. Additionally, it is assumed that PMUs are the only source of these values. Since PMUs are costly equipment that cannot be installed on all busbars, the positions in which they are installed are very crucial. As a result, the placement of PMUs should be optimized in such a way that the greatest possible amount of network observability can be attained with the fewest possible PMUs [29]. The placement and number of PMUs depend on the specification of the system operating state of every case study. It is assumed that the minimum number of PMUs is installed to guarantee full network observability. However, in cases such as communication congestions, short-circuit faults, or cyber-physical attacks on the power system, there is a possibility of PMU missing data. To ensure full observability of the power system, if a PMU is lost, the problem constraints must be changed so that each of the buses can be observable by at least one other PMU [30]. Therefore, in the case of PMU missing data, they are recovered by using other PMUs and network graphs with acceptable accuracy [31]. Since the estimation of missing data has a very small percentage of error [32], it does not affect the stability assessment of the proposed method.

Generally, total vector error (TVE) is regarded as the difference between the synchrophasor estimates obtained from a PMU and the corresponding reference values that are established by evaluating the calculations shown in [33]. After the system is exposed to such measurement errors, the performance of the suggested technique is evaluated, which reveals its high efficiency and resilience against measurement errors. Therefore, the placement of PMUs may be regarded as a preprocessor for this research, while the provided technique is unaffected.

After determining the best locations for the PMUs, the suggested technique specifies the main and backup pairs in the transmission lines. This allows the load currents and short-circuit currents to be computed as they travel through the relays. First, a calculation is made to determine the maximum load current traveling through each relay. In this scenario, the I_{pu} of DOCRs is estimated to be the maximum load current multiplied by 1.5. The pickup current does not factor into the decision-making process. Then, the preliminary data required to solve the problem of optimal coordination between DOCRs is given. This is accomplished by computing the fault current which flows through each of the main relays as well as its corresponding backup relay for faults occurring in front of the near-end and far-end in relation to the primary relay. Finally, the optimization is handled by LP with the minimization of the fitness function presented in previous sections, and the optimum T values are derived from those results for each DOCR.

Once the optimization process is completed and applied to each relay, T and I_{pu} can ensure that DOCRs will operate to their full potential in terms of the disconnection accuracy of faulty parts and speed in the face of any potential fault. Following this stage, one will have the necessary information obtained from the PMUs, and the information can be utilized as a feature vector to WLS-SVM in terms of the active and reactive power, voltage amplitude, and phase angle. In contrast, previous studies could only use one of the aforementioned parameters or a combination of them as the input data category, without being able to consider the effects of other parameters on the transient stability. Therefore, the values are computed for i_{TSI} corresponding to each of these variables and are used as the target data. Then, to assess the performance of the presented approach, 1000 various operating points are produced for the training and testing of WLS-SVM by simulating faults on 20%, 40%, 60%, and 80% of every power line in the case study system, while simultaneously simulating the consecutive load flows. This is because both short-circuit and load flow data are considered to be the input data, contrary to the suggestions of previous studies, this paper includes both the information of the steady-state condition in the power grid in the datasets and the data that the system has been subjected to disturbances. For this reason, the proposed method works much better than other methods. In addition, the operation of DOCRs is taken into account in the production of various operation points for the training of WLS-SVM. For example, at overload of 1.2 times the nominal load, the DOCRs operate, and this is included in the training data of such cases, especially when the configuration of the system changes. Moreover, the training data take into account the short-circuit faults in different parts of the network, which are among the worst cases to occur in the power system. When a short-circuit occurs, the DOCRs operate in disturbance situations, and these operation conditions are considered in the training data.

Ninety percent of the generated data are regarded as the training data which are chosen at random, and the rest of them are considered as the testing data. In addition, PCA is used for reducing the dimensionality of the input datasets and extracting the features of those datasets to render the suggested technique suitable for a real large-scale power system. Since PCA removes the correlated factors that do not affect decision-making, the WLS-SVM algorithm demonstrates improved performance. WLS-SVM is then trained by means of the training data, which is conducted using 10-fold cross-validation to determine the best values of γ and σ. Finally, the WLS-SVM performance is tested by

predicting i_{TSI} on 100 unknown data during the test phase.

In this study, several performance evaluation metrics are used to compare the performance of different prediction methods, presented as:

$$e_{\mathrm{RMSE}}=\sqrt{\frac{1}{n}\sum_{i=1}^{n}(y_i-y_{\mathrm{P}_i})^2} \tag{15}$$

$$e_{\mathrm{MAPE}}=\frac{1}{n}\sum_{i=1}^{n}\left|\frac{y_i-y_{\mathrm{P}_i}}{y_i}\right| \tag{16}$$

$$U=\frac{\sqrt{\frac{1}{n}\sum_{i=1}^{n}(y_i-y_{\mathrm{P}_i})^2}}{\sqrt{\frac{1}{n}\sum_{i=1}^{n}(y_i-\bar{y})^2}} \tag{17}$$

$$d=1-\frac{\sum_{i=1}^{n}(y_i-y_{\mathrm{P}_i})^2}{\sum_{i=1}^{n}(|y_i-\bar{y}|+|y_{\mathrm{P}_i}-\bar{y}|)^2} \tag{18}$$

$$R=\frac{\sum_{i=1}^{n}(y_i-\bar{y})(y_{\mathrm{P}_i}-\bar{y}_{\mathrm{P}})}{\sqrt{\sum_{i=1}^{n}(y_i-\bar{y})^2(y_{\mathrm{P}_i}-\bar{y}_{\mathrm{P}})^2}} \tag{19}$$

where e_{RMSE} presents as the root mean squared error; e_{MAPE} is the mean absolute percentage error; U denotes the Theil's U statistic; d is the Willmott's index of agreement; the correlation coefficient is expressed as R; n presents the total number of samples; y represents the target values; y_{P} represents the predicted ones for each sample; and the means of observed and predicted values are denoted by $\bar{y}$ and $\bar{y}_{\mathrm{P}}$, respectively.

It is worth mentioning that the e_{RMSE} and e_{MAPE} values should be near zero as far as possible for the prediction to be accurate. Furthermore, smaller value for U indicates better performance of the method in prediction, while the values of R and d should be as near to one as possible to ensure the highest accuracy in prediction.

To assess the robustness of the proposed model against a wide array of power system disturbances, an extensive contingency analysis should be conducted for the simulation of various line and generator outages, as a truly robust model must be capable of accurately predicting the system behavior under both typical and extreme conditions. Accordingly, this paper analyzes 41-line contingencies and 6-generator contingencies, encompassing scenarios from minor line outages to significant generator failures, thus covering a broad spectrum of potential power system disturbances. Figure 2 shows the flow diagram of the proposed technique.

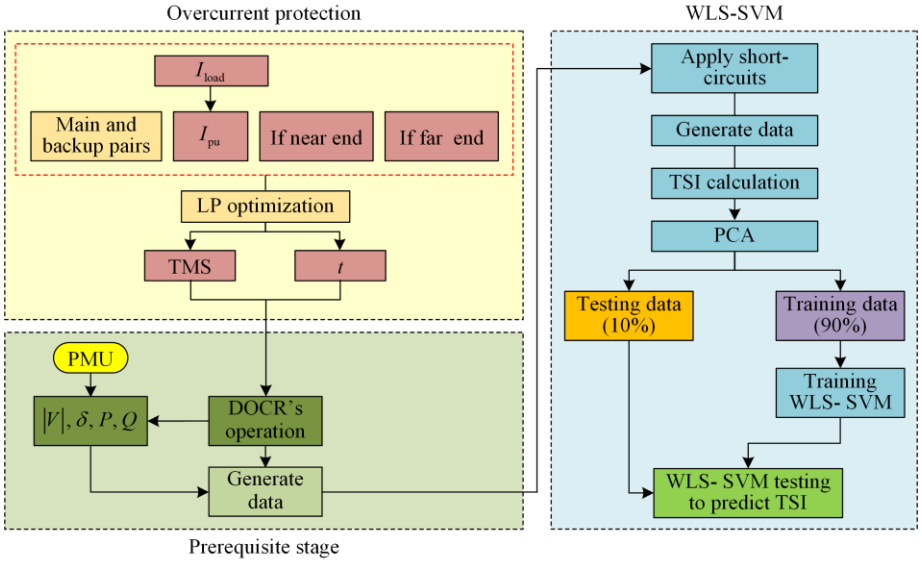

Fig. 2. Flow diagram of the proposed method.

V. Results and Discussion

WLS-SVM has been implemented on both the New England 39-bus system and the IEEE 118-bus system to demonstrate its success in real-time transient stability assessments. In addition, the suggested technique is evaluated alongside ELM, ANFIS, and BPNN. The comparison is carried out by using a wide variety of performance measures, statistical analyses, training times, and testing times. The followings are a more in-depth overview of each of the methods discussed above.

1) ELM is a solution which has been introduced to address the challenges presented by traditional algorithms during the training processes of both single-layer and multiple-layer feed-forward neural networks. It is more efficient and produces better generalizations, as compared to BPNNs. Randomization of the feed-forward neural network weights and biases underlies ELM's operational methodology. For the hidden layer output matrix, this study utilizes the RBF activation function. Additionally, there are a total of 20 neurons.

2) ANFIS is a combination of ANNs and fuzzy system, which aims to enhance the learning process. The selection of the appropriate fuzzy inference system is the characteristic feature of ANFIS design that bears the most weight. In this study, fuzzy rules are generated by the use of the subtractive clustering approach, and 0.4 is considered for the radius of influence.

3) BPNN is one of the most popular types of ANNs, which is often employed to handle nonlinear problems. These types include one input layer, one or more hidden layers, and one output layer. In the present study, the neural network undergoes training for a total of up to 100 epochs. We have assumed that the momentum constant is 0.9, the training rate is 0.01, and there are five neuronal layers excluding the two hidden levels. Additionally, a sigmoid activation function is utilized for BPNN.

A. IEEE 39-bus System

Figure 3 illustrates the IEEE 39-bus system, also known as the New England 39-bus system, which consists of 10 generators and 46 lines. For differentiating the DOCRs from the other components of the power system, the DOCRs are color-coded in red.

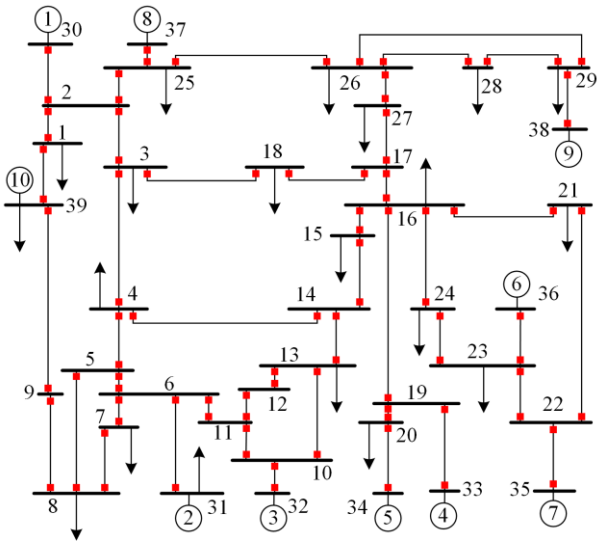

Fig. 3. The New England 39-bus system.

The findings of the presented methodology are evaluated and discussed in conjunction with those of ELM, ANFIS, and BPNN, since the training data of all models are equal. As mentioned in the previous section, datasets for the training and test stages have been produced by simulating three-phase short-circuit faults on each transmission line at 20%, 40%, 60%, and 80% of the line's length while applying 1.1, 1.2, and 1.3 times the load of the line's nominal capacity, respectively. Out of these 1000 examples, 900 are chosen at random to serve as the training data, and the other 100, which have not been seen, are regarded as the testing data.

Accordingly, LP is used to achieve the most effective coordination possible amongst the DOCRs. The optimum values of T are discovered, while the total amount of time that DOCRs have been operational, t_{op}, is 56.2573.

1) The Impact of DOCRs on Transient Stability Assessment

The present study deals with the functioning of the power system protection relays after the incidence of a fault, which leads to the separation of the faulty portion from the remainder of the network, as well as their impact on the transient stability. Up until very recently, transient stability has been evaluated in a manner that is independent of DOCRs' operation. However, protection relays will operate in real-world power systems that make use of DOCRs in the event of a disturbance, or transmission line overload. On the other hand, if there is no protection in place, a disruption in the electrical system can result in a chain reaction of failures and power outages. Therefore, power system stability studies which do not take protective mechanisms into account will be unable to provide a thorough analysis of the real-time transient stability in an actual power grid, and thus cannot provide meaningful results. The present study conducts two different simulations to demonstrate the influence of DOCRs on the evaluation of transient stability:

Scenario 1: This scenario is a stable case, in which the fault is applied to busbar 3 at 2 s, and then, after 0.2 s, the fault is cleared.

Scenario 2: This scenario is an unstable case, in which the fault is applied to busbar 3 at 2 s, and then, after 0.5 s, the fault is cleared.

In both scenarios, the evolution of the variables affecting transient stability, namely the rotor angle of the generators, δ_{max}, and the transient stability assessment index, i_{TSI}, in the presence and absence of overcurrent protection in the pre-fault, during-fault, and post-fault periods, are shown in Figs. 4–6.

Figure 4 compares the variations of variables over time with and without DOCRs for Scenario 1. In Figs. 4 (a) and (b), the rotor angles δ_{rotors}, and δ_{max} without DOCRs are shown, while the same variables are shown in the presence of DOCRs in Figs. 4 (c) and (d), respectively. The transient stability assessment index i_{TSI} as a result of the application of Scenario 1 disturbance with and without DOCRs is shown in Fig. 6 (a), with the time interval of 2 s to 3 s enlarged at the bottom for better clarity. In this scenario, the system is stable in the presence or absence of DOCRs due to the positive value of i_{TSI}, whereas such effect has not been considered in previous studies.

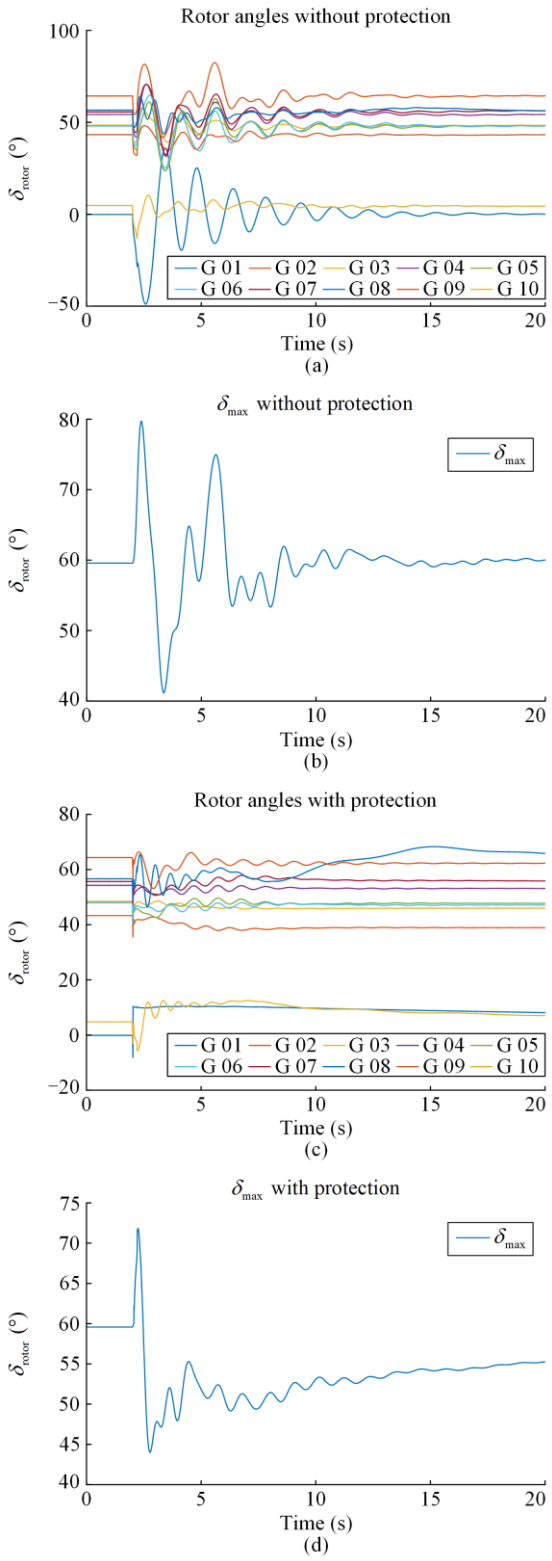

Fig. 4. The evolution of the variables in Scenario 1. (a) δ_{rotors} without DOCRs. (b) δ_{max} without DOCRs. (c) δ_{rotors} with DOCRs. (d) δ_{max} without DOCRs.

In Fig. 5, the status of the parameters for Scenario 2 is shown, and transient monitoring of i_{TSI} with and without DOCRs for this scenario is shown in Fig. 6(b). As can be seen, in the absence of DOCRs, the system becomes unstable after the occurrence of the disturbance with i_{TSI} being negative, while the system remains stable in the presence of DOCRs.

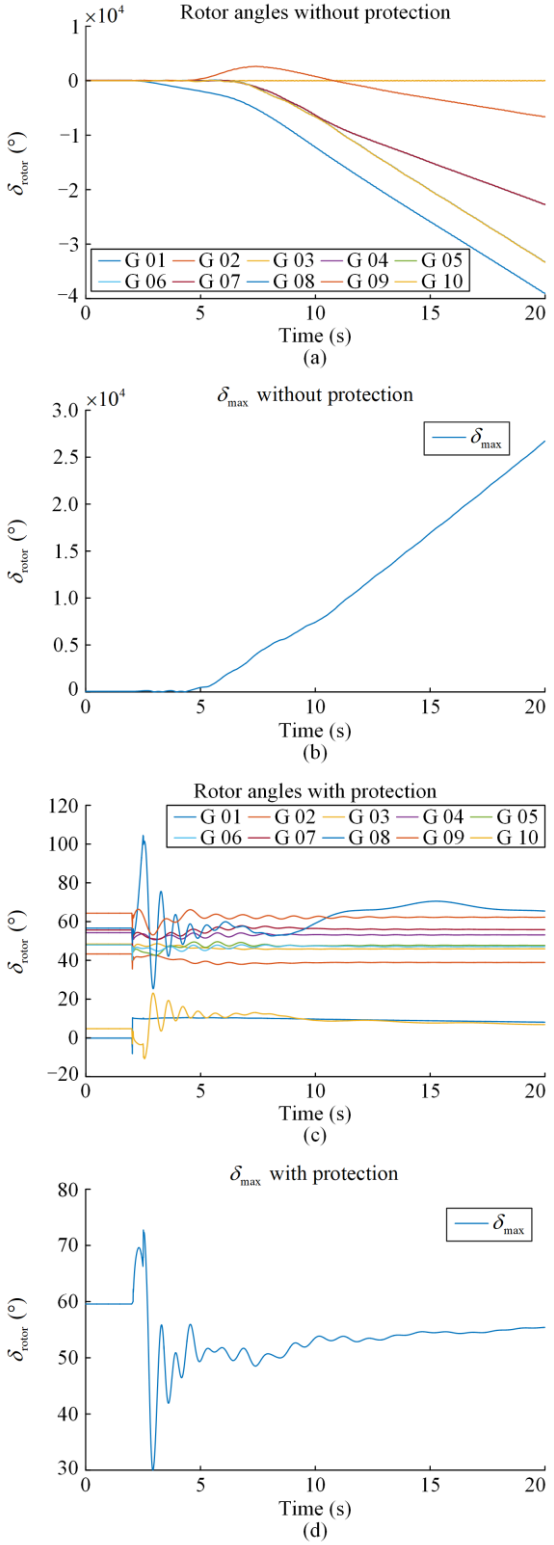

Fig. 5. The evolution of the variables in Scenario 2. (a) δ_{rotors} without DOCRs. (b) δ_{max} without DOCRs. (c) δ_{rotors} with DOCRs. (d) δ_{max} without DOCRs.

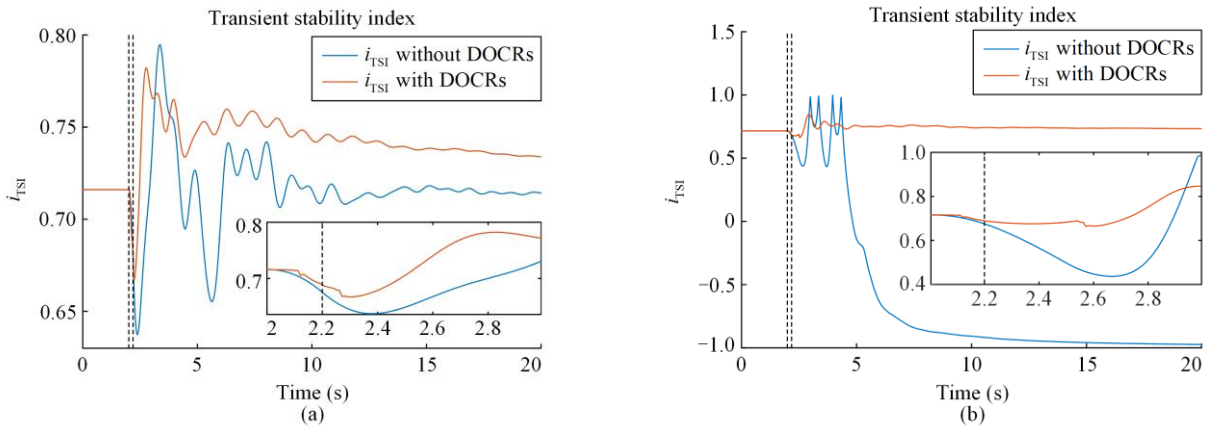

Fig. 6. i_{TSI} with and without DOCRs. (a) Scenario 1. (b) Scenario 2.

As mentioned above, the present study deals with the impact of DOCRs on the transient stability assessment. In previous studies, the effect of relay operations has not been considered, which can cause incorrect evaluation of power system stability. To verify the effect of an overcurrent protection scheme on the transient stability assessment, WLS-SVM is trained in the presence and absence of DOCRs. The actual values and the predicted ones obtained from WLS-SVM are compared for training and testing data with or without DOCRs for the estimation of i_{TSI}, as shown in Fig. 7. Moreover, a comparison of performance indices for estimating i_{TSI} in terms of training and testing data using WLS-SVM with and without DOCRs is also shown in Table I. As seen in Table I, the method proposed with the presence of DOCRs is superior to that in the absence of DOCRs in terms of prediction accuracy.

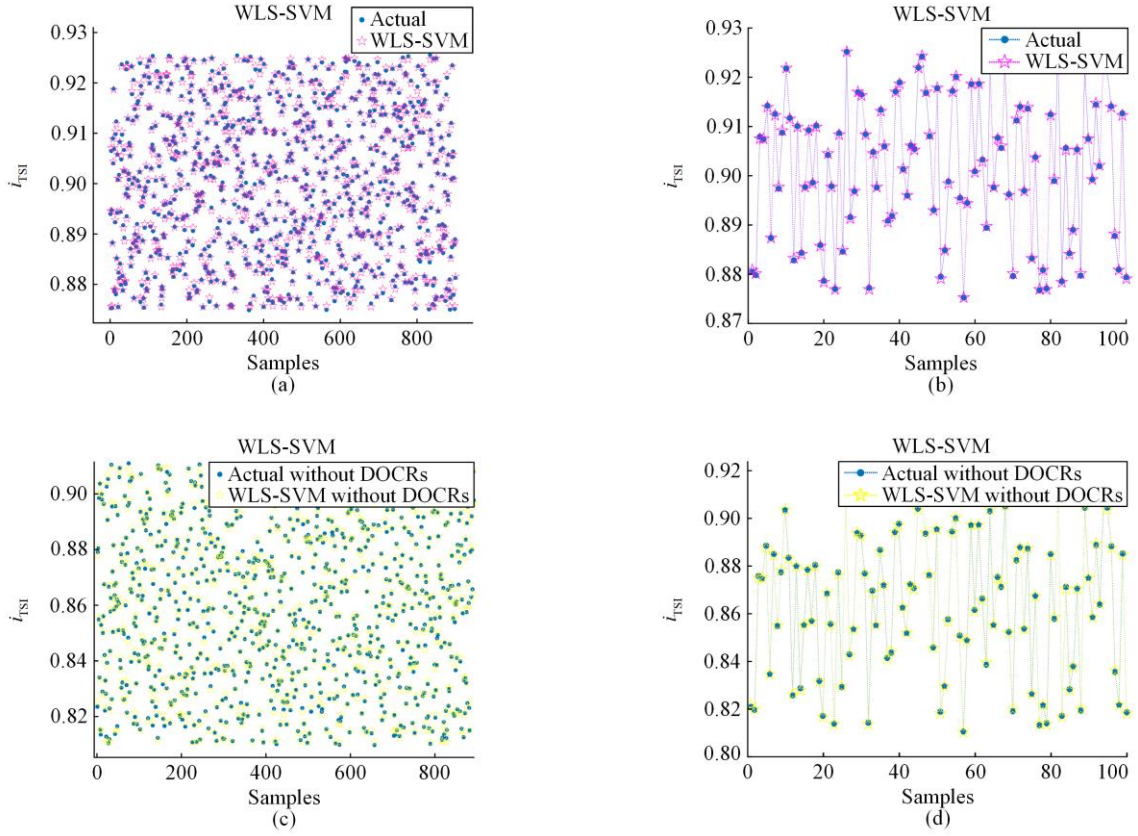

Fig. 7. The actual values vs. the predicted values of i_{TSI} using WLS-SVM. (a) With DOCRs in training data. (b) With DOCRs in testing data. (c) Without DOCRs in training data. (d) Without DOCRs in testing data.

TABLE I
THE PERFORMANCE METRICS IN THE PRESENCE AND THE ABSENCE OF DOCRS USING WLS-SVM

Performance indices	With DOCRs		Without DOCRs	
	Training	Testing	Training	Testing
e_{RMSE}	1.7405×10^{-4}	2.6957×10^{-4}	1.8109×10^{-4}	2.7704×10^{-4}
e_{MAPE}	0.0211	0.0255	0.0215	0.026
U	0.0121	0.0184	0.0134	0.1891
d	0.9999	0.9999	0.9999	0.9999
R	0.9999	0.9998	0.9999	0.9998

2) Impact of Input Vector to WLS-SVM on Prediction Accuracy

According to power flow equations, changes in the active power, P, and the reactive power, Q, are less sensitive to changes in the voltage magnitude, V, and the voltage phase angle, φ, respectively. For this reason, Q and V parameters are usually used to evaluate the voltage stability, and P and φ the transient stability. Therefore, the effects of Q and V, in addition to those of P and φ, on the transient stability, should be examined more closely. Thus, the present study takes into account P, Q, V, and φ as the input vector to WLS-SVM. It should be noted that considering all the parameters P, Q, V, and φ simultaneously creates high-dimensional data, which significantly increases the computational burden and can reduce the accuracy of the prediction. To reduce the dimension of input data to WLS-SVM, PCA is implemented. To show the effect of considering the parameters P, Q, V, and φ as the input data, rather than only Q and V or P and φ, Table II shows the accuracies of the proposed method with the above-mentioned inputs in the training data.

TABLE II
THE PERFORMANCE INDICES IN TRAINING DATA WITH DIFFERENT PARAMETERS AS INPUT DATA

Performance indices	V, φ, P, Q	V, Q	φ, P
e_{RMSE}	1.7405×10^{-4}	0.001	4.2961×10^{-4}
e_{MAPE}	0.0211	0.0801	0.0365
U	0.0121	0.0695	0.0299
d	0.9999	0.9987	0.9999
R	0.9999	0.9995	0.9998

As can be seen from Table II, by considering all the parameters P, Q, V, and φ, the mutual effects of the voltage stability and transient stability can be considered, and consequently, the accuracy of the proposed method is improved.

To demonstrate the efficacy of PCA, Table III analyzes the proposed method with and without PCA. As can be seen, considering all the parameters significantly increases the training and testing times of the network. However, the prediction accuracy does not bring noticeable change, compared to the case where PCA is used as a tool to extract features and reduce dimensions for preventing the overfitting of the model. Moreover, it is worth mentioning that due to the nature of SVMs, the number of samples and feature vectors can lead to an increase in their training and testing times, whereas using PCA can solve this problem.

TABLE III
ANALYZE THE EFFECTIVENESS OF PCA IN TERMS OF REDUCING THE DIMENSIONALITY OF INPUT VECTORS

Input parameters	Time (s)		Performance indices		
	Training	Testing	e_{RMSE}	e_{MAPE}	R
V, φ, P, Q + PCA	0.4118	0.0029	1.7405×10^{-4}	0.0211	0.9999
V, φ, P, Q	0.8506	0.0059	1.7514×10^{-4}	0.2137	0.9999

3) Contingency Analysis

Contingency analysis is conducted to demonstrate the WLS-SVM model's remarkable resilience and predictive accuracy across a multitude of scenarios. For line contingencies, the model manages to maintain high predictive accuracy, with the power losses ranging from 128.76 MW to 179.88 MW and the reactive power losses varying significantly, highlighting the model's ability to adapt to different disturbance magnitudes and types. Among the generator contingencies analyzed, one scenario is identified where the model fails to provide a solution, pinpointing an extreme condition beyond the system's operational limits. This particular case has been instrumental in identifying the current capabilities of the proposed method. Moreover, it serves as a critical focal point for subsequent model refinements.

To further illustrate the model's robustness, the failed generator contingency scenario is dissected, uncovering valuable insights into the limitations inherent in the proposed modeling approach. This rigorous analysis forms the basis for ongoing enhancements aimed at increasing the model's sensitivity and accuracy, especially under extreme conditions. The learnings from this scenario directly contribute to the iterative improvement of the proposed model, ensuring not only enhanced robustness but also superior generalization capabilities across a wider array of power system disturbances.

4) Comparison and Discussion

To evaluate WLS-SVM against the other three approaches, all methods must first be trained while being assessed with the test data. The obtained hyperparame-

ters for the IEEE 39-bus system are γ=2421.2696 and σ^2=2451.2677. When trying to estimate i_{TSI} while taking DOCRs into account and without having measurement errors play a factor, the actual and estimated ones for the train datasets are compared. In addition, to estimate i_{TSI} for the training data while accounting for DOCRs and eliminating the measurement errors, Table IV gives an examination of the performance metrics.

It show that the new approach has superiority over other methods in terms of the accuracy of its predictions. In contrast to the other approaches, WLS-SVM has the lowest values for e_{RMSE}, e_{MAPE}, and U, while it also has values in d and R very similar to 1.

TABLE IV
THE PERFORMANCE METRICS OF ALL MODELS IN THE PREDICTION OF TRANSIENT STABILITY INDEX WITH DOCRS IN TRAINING DATA

Performance indices	WLS-SVM	ELM	ANFIS	BPNN
e_{RMSE}	1.7405×10^{-4}	0.0009	0.0012	0.0014
e_{MAPE}	0.0211	0.0966	0.1028	0.1589
U	0.0121	0.0626	0.0834	0.0973
d	0.9999	0.999	0.9986	0.9979
R	0.9999	0.9998	0.999	0.9971

5) Effect of the Measurement Error of PMUs

The influence of errors is evaluated on both the training and test datasets to show the resilience of the proposed technique in the presence of PMU measurement errors. TVE under the steady-state operation must be lower than 1% to comply with the IEEE standard 60255-118-1-2018 [33]. It should be noted that the value of TVE is reduced to less than 1% when there is a phase error of 0.57 degrees, which is comparable to 0.01 radians or an amplitude error of 1% for the 60 Hz system. For this reason, TVE is applied not only to the feature vectors but also to the predictor vectors. Table V and Table VI provide, respectively, the performance indicators that are compared in estimating i_{TSI} in the presence and absence of measurement errors for test data by DOCRs with different approaches. The findings show that the measurement errors have rather little impact on the suggested technique, which functions well even in an environment with noise or with PMU measurement errors.

TABLE V
THE PERFORMANCE METRICS WITHOUT MEASUREMENT ERROR IN TESTING DATA

Performance indices	WLS-SVM	ELM	ANFIS	BPNN
e_{RMSE}	2.6957×10^{-4}	0.0012	0.0014	0.0016
e_{MAPE}	0.0255	0.1112	0.139	0.1707
U	0.0184	0.0819	0.0956	0.1093
d	0.9999	0.9983	0.9977	0.9966
R	0.9998	0.9993	0.9988	0.997

TABLE VI
THE PERFORMANCE METRICS WITH MEASUREMENT ERROR IN TESTING DATA

Performance indices	WLS-SVM	ELM	ANFIS	BPNN
e_{RMSE}	0.0037	0.0066	0.0057	0.0058
e_{MAPE}	0.3559	0.6852	0.5651	0.5758
U	0.2163	0.3858	0.3332	0.339
d	0.9117	0.9068	0.8871	0.8887
R	0.9988	0.9922	0.9937	0.966

6) Correlation Plot

How closely two variables are connected linearly is measured by means of a statistical concept known as "correlation". In regression problems, the correlation between the targets and their corresponding predictions is expressed through the correlation coefficient, which is denoted as R in this paper. Moreover, the scatter diagram, called the correlation plot, demonstrates the linear correlation between the actual values on the horizontal axis versus the predicted values on the vertical axis. The correlation plots for all four methods to estimate i_{TSI} in the testing phase with the measurement errors are depicted in Fig. 8.

In Fig. 8, the linear correlation between the target values and the estimated ones is depicted in bold line, while the dotted line depicts the actual values equal to the predicted values. Ideally, the actual values and the predicted values should be equal. Therefore, for a high-accuracy model, the bold line and the dotted line will precisely coincide or be approximately close to coinciding with each other, while all predicted values are mapped on the dotted line. In summary, the dotted line in Fig. 8 represents the line on which the line of real and predicted values is equal, while the bold line represents the linear regression between the actual and predicted values. In light of the above-mentioned facts, the bold line and the dotted line are almost overlapped in the proposed method, as shown in Fig. 8(a), which means that the proposed method is superior to other methods.

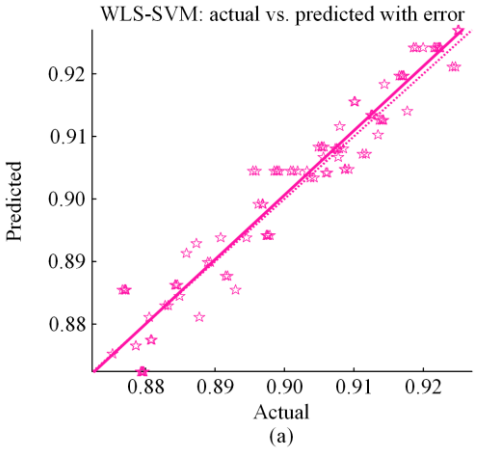

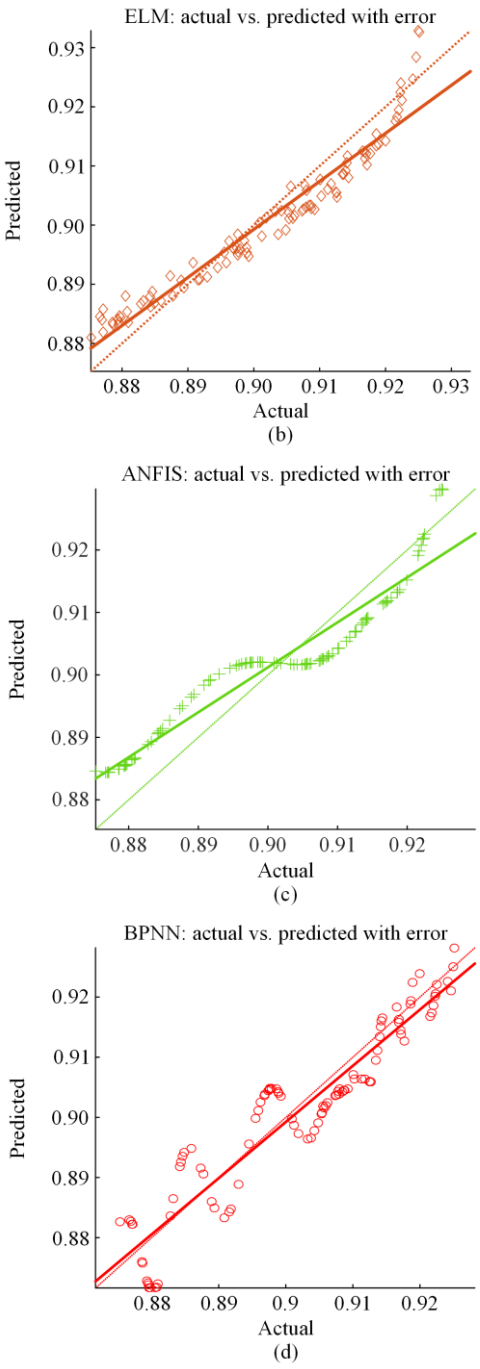

Fig. 8. Correlation plots of actual values and predicted values of i_{TSI} in testing data with measurement error. (a) WLS-SVM. (b) ELM. (c) ANFIS. (d) BPNN.

7) Discrepancy Ratio

Discrepancy ratio (DR) is one of the performance evaluation indicators for the comparison of prediction models in terms of accuracy. This index is calculated by dividing the predicted values with the actual values for each sample. The closer the DR of different samples to 1, the higher the performance of the prediction model in estimating the actual value in that sample. Therefore, to compare the four models in terms of prediction accuracy, the DR diagram is drawn for each sample in Fig. 9. As can be seen, the values of DR for WLS-SVM are closer to 1 than the others, which indicates higher accuracy of this method.

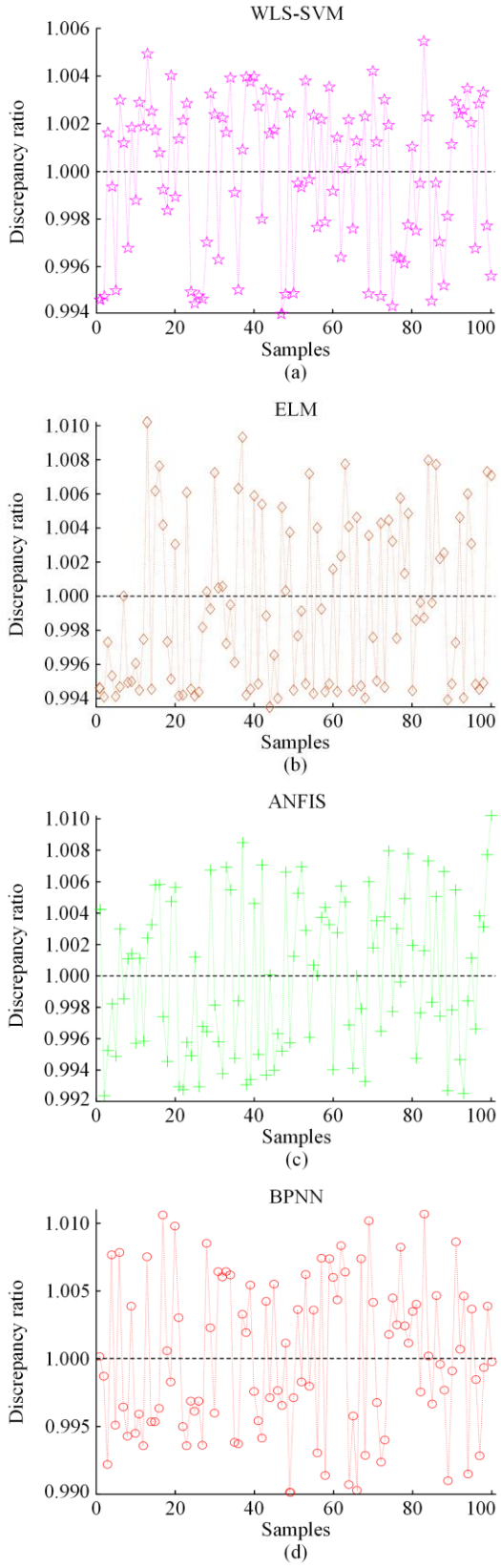

Fig. 9. Discrepancy ratio of i_{TSI} in testing data with measurement error. (a) WLS-SVM. (b) ELM. (c) ANFIS. (d) BPNN.

Table VII presents the maximum, minimum, and average e_{DR} (DR values) for the four methods. As shown, the WLS-SVM method has less deviation around e_{DR}=1 , with the highest $e_{DR,\,min}$ and lowest $e_{DR,\,max}$ of 0.994 and 1.0055, respectively, while $e_{DR,\,avg}$ is equal to 0.9999, which is very close to 1. This shows that the average performance of the proposed method is very close to the actual value, indicating the high efficiency of WLS-SVM.

TABLE VII
THE MAXIMUM, MINIMUM, AND AVERAGE VALUE OF DR

Index	WLS-SVM	ELM	ANFIS	BPNN
$e_{DR,\,min}$	0.994	0.9933	0.9924	0.9902
$e_{DR,\,avg}$	0.9999	0.9994	1.0001	1.0001
$e_{DR,\,max}$	1.0055	1.0106	1.0102	1.0107

8) Regression Receiver Operating Characteristic Curve

The regression receiver operating characteristic (RROC) curve shows over-estimation, rather than under-estimation, to assess the prediction's accuracy of various models. Additionally, the area over the RROC curve, known as the area over curve [34], is an index derived from the RROC curve, and as this value decreases the model's accuracy increases. The RROC curve and the area over curve are conceptualized and shown in Fig. 10(a). Figure 10(b) depicts the RROC curve calculated by means of all four models to evaluate the data while taking into account DOCRs and measurement errors. The smaller value of the area over RROC curve, A, for a model, the more accurate the model in prediction. The A values for various models' predictions of i_{TSI} in the presence of DOCRs and with the measurement errors for the testing data are shown in Table VIII. As can be seen, the proposed method has the lowest A value, which indicates its superiority to the rest of the models in terms of accuracy.

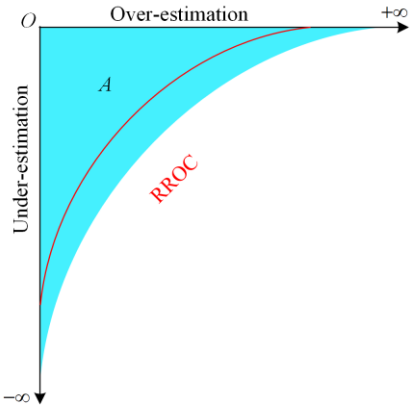

(a)

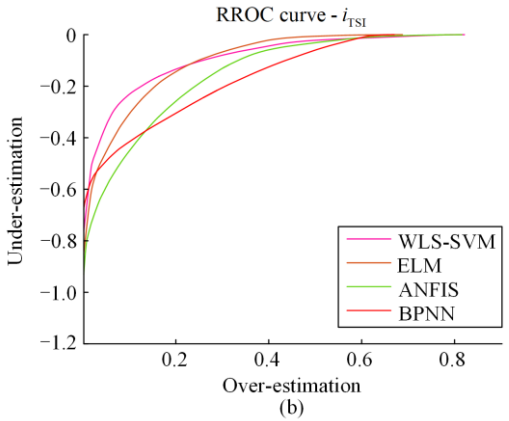

(b)

Fig. 10. Area over RROC curve. (a) The concept. (b) RROC curve of all methods with measurement error.

TABLE VIII
AREA OVER CURVE OF VARIOUS TECHNIQUES FOR TESTING DATA WITH MEASUREMENT ERROR IN TESTING DATA

Performance index	WLS-SVM	ELM	ANFIS	BPNN
A	0.0692	0.0961	0.1316	0.1411

9) Overview

In conclusion, Fig. 11 provides a visual representation of how well each of the four models performs in forecasting i_{TSI} by comparing various indices using a bar diagram. Since the e_{RMSE} value is lower than the values of the other indices, it is measured by means of the left y-axis, while the other indices are compared through the right y-axis. As clearly shown in Fig. 11, WLS-SVM has the lowest value among the four models in e_{RMSE} , e_{MAPE} , U, and A, and the largest values of R and d, which shows the superiority of the proposed method in high accuracy and optimal efficiency as an online method for evaluating the transient stability in real power systems.

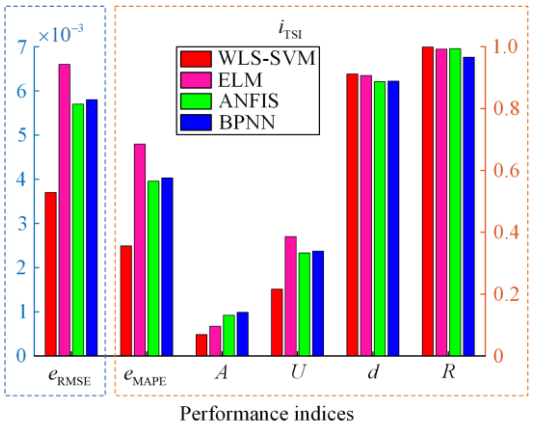

Fig. 11. Comparison between various performance indices.

B. IEEE 118-bus System

The IEEE 118-bus system, depicted in Fig. 12, consists of 91 loads, 9 transformers, 177 lines, and 54

generators. Such a big system introduces more challenges in the assessment of transient stability, which calls for a powerful and robust method like the proposed WLS-SVM to predict i_{TSI} accurately. In our comprehensive analysis, all four models' training and testing data are produced by introducing faults to 20%, 40%, 60%, and 80% of length of lines at nominal load multiplied by 1.05, 1.1, and 1.15, respectively, until power flow converges. Moreover, LP is used to achieve the most effective and efficient coordination of DOCRs, ensuring the proper operation of DOCRs in response to severe disturbances. The total operating times of all the DOCRs in the system, t_{op}, add up to 189.9529 s, and there is a t_{CTI} of 0.2 s between the operations of the primary and backup relays for locating the best answer.

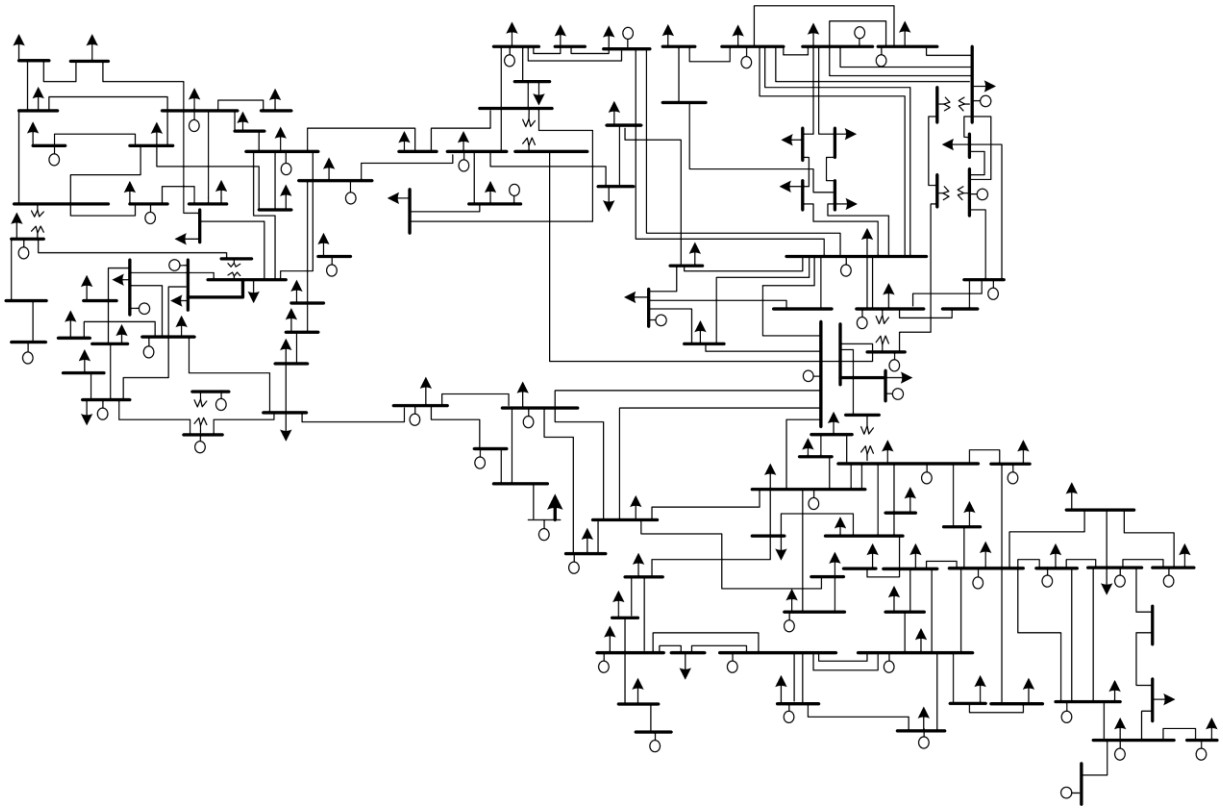

Fig. 12. The IEEE 118-bus system.

After the WLS-SVM and other three approaches have been trained on the given datasets, they are subjected to testing. After training the WLS-SVM, the optimal values are obtained as $\gamma = 1055.5112$ and $\sigma^2 = 7.8028$, ensuring that the proposed WLS-SVM is fit for the dynamics of the IEEE 118-bus system. The findings of both training and testing phases for estimating i_{TSI} are shown in Table IX and Table X, respectively. The tables and other performance metrics, consider the measurement errors as well as the existence of DOCRs. As shown, similar to the performance of the proposed method in the 39-bus system, in the IEEE 118-bus system, WLS-SVM shows a much better performance than other methods, demonstrating that the proposed method not only handles different configurations with more complexities but also shows its accuracy in i_{TSI} prediction under various fault scenarios for the training and test datasets. WLS-SVM has the lowest value of e_{RMSE}, e_{MAPE}, and A among all the four models, which indicates its high accuracy. Moreover, the lowest value of U validates the accuracy of the proposed model, while the highest values of R and d, which are very close to 1, show the absolute superiority of the proposed method over the other three used methods.

TABLE IX
THE PERFORMANCE INDICES IN TRAINING DATA IN THE IEEE 118-BUS SYSTEM

Performance indices	WLS-SVM	ELM	ANFIS	BPNN
e_{RMSE}	0.0025	0.003	0.0039	0.0066
e_{MAPE}	0.2143	0.2506	0.4321	0.581
U	0.0513	0.0616	0.0801	0.1356
d	0.9624	0.9511	0.9481	0.9304
R	0.9997	0.9987	0.9991	0.9911
A	0.0224	0.0462	0.0486	0.2341

TABLE X
THE PERFORMANCE INDICES IN TESTING DATA IN THE IEEE 118-BUS SYSTEM

Performance indices	WLS-SVM	ELM	ANFIS	BPNN
e_{RMSE}	0.0031	0.0034	0.0045	0.007
e_{MAPE}	0.2575	0.274	0.4546	0.6047
U	0.0684	0.0751	0.0993	0.1545
d	0.9319	0.9187	0.9014	0.8655
R	0.9994	0.9983	0.9986	0.9903
A	0.0243	0.0484	0.0498	0.2363

The computational efficiency of WLS-SVM, as shown in Table XI, is well fit for real-time application as a major development in transient stability assessment for complex power systems such as the IEEE 118-bus system. This efficiency, in combination with accuracy, makes the WLS-SVM model a very pivotal tool for the reliability and security of modern power networks.

C. The Consumed Time in Training and Testing

The amount of time required for training and testing each approach is computed on a computer with the specifications Intel® Core™ i7-4510U CPU running at 2 GHz. At the same time, on the same machine, each of the approaches undergoes training and testing. The amount of time required to compute the training and testing stages of all four approaches is outlined in Table XI for both the IEEE 39-bus and 118-bus systems. According to Table XI, the presented technique completes the training and testing stages more quickly than the existing methods, which indicates that it is appropriate for implementing in real-time power system applications.

TABLE XI
THE CONSUMED TIME IN THE TRAINING AND TESTING PROCESS

Methods	Training time (s)		Testing time (s)	
	39-bus	118-bus	39-bus	118-bus
WLS-SVM	0.4118	1.0323	0.0029	0.0096
ELM	0.5863	1.8944	0.0031	0.0151
ANFIS	0.7496	2.215	0.0056	0.0211
BPNN	0.8822	3.0076	0.0063	0.0374

D. Discussion

This section compares and discusses the existing methods for evaluating the transient stability in recent years. Accuracy is one of the most important parameters, which has a critical impact on the online and real-time assessment of the stability of power systems. In this case, references [23] and [24] provide high accuracy, closely matching the performance of the proposed method, while references [26], [16], and [22] have limited accuracy. Additionally, references [23], [24], and [26] require a large amount of memory, while references [16], [22] and the proposed method require low memory. In terms of computational burden, references [23] and [26] have a high computational load, references [24] and [16] have a moderate computational burden, while the proposed method and reference [22] have a low computational burden. Only the proposed method and reference [26] are resistant to the noisy environments in real power systems. In terms of real-world applications, only the proposed method and reference [23] are suitable. To our knowledge, no study has seriously considered the effect of protection systems, hence the significance of the proposed method. The summary of the above discussions is given in Table XII.

TABLE XII
COMPARISON BETWEEN DIFFERENT APPROACHES OF TRANSIENT STABILITY ASSESSMENT

Parameters	[23]	[24]	[26]	[16]	[22]	Proposed method
Accuracy	High	High	Moderate	Moderate	Moderate	High
Memory	High	High	High	Low	Low	Low
Computational burden	High	Moderate	High	Moderate	Low	Low
Robustness to noise	×	×	√	×	×	√
Real-world application	√	×	×	×	×	√
Protection system impact	×	×	×	×	×	√

VI. CONCLUSION

This study has validated that the WLS-SVM method is capable of real-time assessment of transient stability, including the highly important aspect of overcurrent protection. The proposed approach careful considers the dynamic interactions involving protective relays and system stability, while optimizing DOCR coordination through LP for the globally optimal operating times.

It has demonstrated that the proposed method leads to better accuracy in the prediction, as it provides a complete feature vector including active and reactive powers, voltage amplitudes, and phase angles, in addition to validation for input data dimensionality reduction with PCA. The computational efficiency has been found to be comparable with the ELM, ANFIS, BPNN methods, while its prediction accuracy is superior to those methods across all the benchmark datasets for the New England 39-bus and the IEEE 118-bus systems. Generally, WLS-SVM has the smallest values of A, e_{RMSE}, e_{MAPE}, and U, as compared to the other methods, which shows its very discriminative power in differentiating stable condition from unstable condition with minimal

error. Highest values of R and d near unity also demonstrate that the model has a very high precision for predicting the transient stability indices. Essentially, this shows the abilities of the WLS-SVM model in enhancing the prediction accuracy of transient stability, with high efficiency in solving operational dynamics of DOCRs.

This work provides a basis for future research focusing on the transient instability times, and at the same time, focusing on the precision of setting up the online training phases, which can enhance power system resilience and reliability.

ACKNOWLEDGMENT

Not applicable.

AUTHORS' CONTRIBUTIONS

Amir Hossein Poursaeed: conceptualization, data curation, methodology, software, validation, visualization, writing and editing. Farhad Namdari: conceptualization, data curation, formal analysis, investigation, methodology, validation, review & editing. Both authors read and approved the final manuscript.

FUNDING

This work is carried out without the support of any funding agency.

AVAILABILITY OF DATA AND MATERIALS

Please contact the corresponding author for data material request.

DECLARATIONS

Competing interests: The authors declare that they have no known competing financial interests or personal relationships that could have appeared to influence the work reported in this article.

AUTHORS' INFORMATION

Amir Hossein Poursaeed received the B.S. and M.S. degrees in electrical power engineering from Lorestan University (LU), Khorram Abad, Iran, in 2015 and 2018, respectively. His research interests include power system protection and stability, electromagnetic transients, renewable integration, and machine learning applications in power systems.

Farhad Namdari received his B.Sc. and M.Sc. degrees in electrical power engineering from Iran University of Science and Technology (IUST) and Tarbiat Modares University in 1994 and 1998, respectively, and his Ph.D. in electrical power engineering from IUST in 2006. In 2009, he joined LU, Iran as an assistant professor, and spent the next more than 14 years there progressing to associate professor in 2015, professor in 2021 until he started the new role within the University of Exeter in January 2024. His fields of interest are power system protection and stability, smart grids, power system transients, power system optimization, and wide area monitoring, protection, and control.

REFERENCES

[1] P. W. Sauer, M. A. Pai, and J. H. Chow, *Power system dynamics and stability: with synchrophasor measurement and power system toolbox*, 2nd ed., New York, USA: Wiley-IEEE Press, 2017.

[2] A. R. Sobbouhi and A. Vahedi, "Transient stability prediction of power system; a review on methods, classification and considerations," *Electric Power Systems Research*, vol. 190, Jan. 2021.

[3] S. Ghosh, Y. J. Isbeih, and S. K. Azman *et al.*, "Optimal PMU allocation strategy for completely observable networks with enhanced transient stability characteristics," *IEEE Transactions on Power Delivery*, vol. 37, no. 5, pp. 4086-4102, Oct. 2022.

[4] L. Zhu, D. J. Hill, and C. Lu, "Hierarchical deep learning machine for power system online transient stability prediction," *IEEE Transactions on Power Systems*, vol. 35, no. 3, pp. 2399-2411, May 2020.

[5] S. M. Mazhari, N. Safari, and C. Y. Chung *et al.*, "A hybrid fault cluster and Thévenin equivalent based framework for rotor angle stability prediction," *IEEE Transactions on Power Systems*, vol. 33, no. 5, pp. 5594-5603, Sept. 2018.

[6] J. Segundo-Ramirez, A. Bayo-Salas, and M. Esparza *et al.*, "Frequency domain methods for accuracy assessment of wideband models in electromagnetic transient stability studies," *IEEE Transactions on Power Delivery*, vol. 35, no. 1, pp. 71-83, Feb. 2020.

[7] J. Wang, J. Liang, and F. Gao *et al.*, "A closed-loop time-domain analysis method for modular multilevel converter," *IEEE Trans Power Electron*, vol. 32, no. 10, pp. 7494-7508, Oct. 2017.

[8] J. Liu, D. Yang, and W. Yao *et al.*, "PV-based virtual synchronous generator with variable inertia to enhance power system transient stability utilizing the energy storage system," *Protection and Control of Modern Power Systems*, vol. 2, no. 4, pp. 1-8, Oct. 2017.

[9] Y. Li and Z. Yang, "Application of EOS-ELM with binary Jaya-based feature selection to real-time transient stability assessment using PMU data," *IEEE Access*, vol. 5, pp. 23092-23101, Oct. 2017.

[10] D. P. Wadduwage, C. Q. Wu, and U. D. Annakkage, "Power system transient stability analysis via the concept of Lyapunov exponents," *Electric Power Systems Research*, vol. 104, pp. 183-192, Nov. 2013.

[11] D. R. Gurusinghe and A. D. Rajapakse, "Post-disturbance transient stability status prediction using synchrophasor measurements," *IEEE Transactions on Power Systems*, vol. 31, no. 5, pp. 3656-3664, Sept. 2016.

[12] J. Lü, M. Pawlak, and U. D. Annakkage, "Prediction of the transient stability boundary using the lasso," *IEEE Transactions on Power Systems*, vol. 28, no. 1, pp. 281-288, Jan. 2013.

[13] P. Sarajcev, A. Kunac, and G. Petrovic *et al.*, "Artificial intelligence techniques for power system transient stability assessment," *Energies*, vol. 15, no. 2, Jan. 2022.

[14] W. Guo, N. M. F. Qureshi, and M. A. Jarwar *et al.*, "AI-oriented smart power system transient stability: the rationality, applications, challenges and future opportunities,"

Sustainable Energy Technologies and Assessments, vol. 56, Mar. 2023.

[15] S. A. Siddiqui, K. Verma, and K. R. Niazi *et al.*, "Real-time monitoring of post-fault scenario for determining generator coherency and transient stability through ANN," *IEEE Transactions on Industry Applications*, vol. 54, no. 1, pp. 685-692, Jan. 2018.

[16] Z. Chen, X. Xiao, and C. Li *et al.*, "Real-time transient stability status prediction using cost-sensitive extreme learning machine," *Neural Computing and Applications*, vol. 27, no. 2, pp. 321-331, Feb. 2016.

[17] T. Behdadnia, Y. Yaslan, and I. Genc, "A new method of decision tree based transient stability assessment using hybrid simulation for real-time PMU measurements," *IET Generation, Transmission & Distribution*, vol. 15, no. 4, pp. 678-693, Feb. 2021.

[18] C. Ren, Y. Xu, and R. Zhang, "An interpretable deep learning method for power system transient stability assessment via tree regularization," *IEEE Transactions on Power Systems*, vol. 37, no. 5, pp. 3359-3369, Sep. 2022.

[19] M. R. Hazari, E. Jahan, and M. A. Mannan *et al.*, "Transient stability enhancement of a grid-connected large-scale PV system using fuzzy logic controller," *Electronics*, vol. 10, no. 19, Oct. 2021.

[20] S. R. Khuntia and S. Panda, "ANFIS approach for SSSC controller design for the improvement of transient stability performance," *Mathematical and Computer Modelling*, vol. 57, no. 1, pp. 289-300, Jan. 2013.

[21] S. Amini, S. Ghasemi, and I. Azadimoshfegh *et al.*, "A two-stage strategy for generator rotor angle stability prediction using the adaptive neuro-fuzzy inference system," *Electrical Engineering*, pp. 1-17, May 2023.

[22] W. Hu, Z. Lu, and S. Wu *et al.*, "Real-time transient stability assessment in power system based on improved SVM," *Journal of Modern Power Systems and Clean Energy*, vol. 7, no. 1, pp. 26-37, Jan. 2019.

[23] Z. Shi, W. Yao, and L. Zeng *et al.*, "Convolutional neural network-based power system transient stability assessment and instability mode prediction," *Applied Energy*, vol. 263, Apr. 2020.

[24] H. Cui, Q. Wang, and Y. Ye *et al.*, "A combinational transfer learning framework for online transient stability prediction," *Sustainable Energy, Grids and Networks*, vol. 30, Jun. 2022.

[25] J. Zhao, Y. Zhang, and P. Zhang *et al.*, "Development of a WAMS based test platform for power system real time transient stability detection and control," *Protection and Control of Modern Power Systems*, vol. 1, no. 1, pp. 1-11, Jul. 2016.

[26] S. Cheng, Z. Yu, and Y. Liu *et al.*, "Power system transient stability assessment based on the multiple paralleled convolutional neural network and gated recurrent unit," *Protection and Control of Modern Power Systems*, vol. 7, no. 3, pp. 1-16, Jul. 2022.

[27] S. V. Khond and G. A. Dhomane, "Optimum coordination of directional overcurrent relays for combined overhead/cable distribution system with linear programming technique," *Protection and Control of Modern Power Systems*, vol. 4, no. 2, pp. 1-7, Apr. 2019.

[28] J. A. K. Suykens, J. De Brabanter, and L. Lukas *et al.*, "Weighted least squares support vector machines: robustness and sparce approximation," *Neurocomputing*, vol. 48, no. 1, pp. 85-105, Oct., 2002.

[29] C. Lu, Z. Wang, and M. Ma *et al.*, "An optimal PMU placement with reliable zero injection observation," *IEEE Access*, vol. 6, pp. 54417-54426, 2018.

[30] M. Esmaili, K. Gharani, and H. A. Shayanfar, "Redundant observability PMU placement in the presence of flow measurements considering contingencies," *IEEE Transactions on Power Systems*, vol. 28, no. 4, pp. 3765-3773, Jul. 2013.

[31] S. Basumallik, R. Ma, and S. Eftekharnejad, "Packet-data anomaly detection in PMU-based state estimator using convolutional neural network," *International Journal of Electrical Power and Energy Systems*, vol. 107, pp. 690-702, May 2019.

[32] Z. Yang, H. Liu, and T. Bi *et al.*, "An adaptive PMU missing data recovery method," *International Journal of Electrical Power and Energy Systems*, vol. 116, Mar. 2020.

[33] IEEE/IEC International Standard-Measuring relays and protection equipment-part 118-1: synchrophasor for power systems-measurements, IEEE/IEC C37.111-2013, 2018.

[34] J. Hernández-Orallo, "ROC curves for regression," *Pattern Recognition*, vol. 46, no. 12, pp. 3395-3411, Dec. 2013.